

Electronic Supplementary Information

“Highly enhanced photoluminescence of rose-like hierarchical superstructure prepared by self-assembly of rare-earth hydroxocation nanosheets and polyoxomolybdate anions”

Byung-Il Lee and Song-Ho Byeon*

*Department of Applied Chemistry, College of Applied Science, Kyung Hee University,
Gyeonggi-do 446-701, Korea.*

e-mail: shbyun@khu.ac.kr (S.-H. B.)

Chem. Commun.

Experimental details; An aqueous colloidal solution was prepared in first by adding 0.10 M KOH solution dropwise to 0.05 M $\text{GdCl}_3 \cdot 6\text{H}_2\text{O}$ and $\text{EuCl}_3 \cdot 6\text{H}_2\text{O}$ solutions with vigorous stirring at room temperature. These solutions, which contain a precipitate, were then heated to 60 °C for 12 h and successively refluxed for 24 h with stirring. The slurries of resulting $\text{Gd}_2(\text{OH})_5\text{Cl} \cdot n\text{H}_2\text{O}$ (LGdH) and $\text{Eu}_2(\text{OH})_5\text{Cl} \cdot n\text{H}_2\text{O}$ (LEuH) were prepared by centrifuging down and washing these precipitates with deionized water. To prepare an aqueous colloidal suspension, the slurry of LGdH and LEuH was ultra-sonicated in deionized water. The LGdH and LEuH were readily dispersed to produce a translucent suspension within 5 min. Such a colloidal solution was mixed with the aqueous anionic solution containing a 2-fold molar excess of sodium molybdate (Na_2MoO_4). After clear solution was formed by uniform stirring, aqueous HCl (1.0 M) solution was added until the pH of solution was adjusted to be in the range of 4 ~ 10. Thus, assembly of defined superstructures was controlled by the pH of the initial aqueous mixture. This mixed solution was kept for a day at room temperature for the self-assembly reaction between hydroxocations and (polyoxo)molybdate anions. The final precipitate (LGdH-Mo and LEuH-Mo) was filtered, washed thoroughly with deionized water, and dried at 40 °C.

Characterization; The chemical compositions of LGdH-Mo and LEuH-Mo were determined by inductively coupled plasma (ICP; Thermo Elemental Thermo ICAP 6000), thermogravimetry (TG; Seiko Instruments TG/DTA320 SSC/5200 S11), and elemental analysis (EA; CE Instruments Flash EA1112). The powder X-ray diffraction patterns were recorded on a rotating anode installed diffractometer (MacScience Model M18XHF). The

Cu K α radiation used was monochromated by a curved-crystal graphite. Field emission scanning electron microscopy (FE-SEM) was carried out with a Carl Zeiss LEO SUPRA 55 electron microscope operating at 30 kV. Specimens for electron microscope were coated with Pt-Rh for 180 s under vacuum. Atomic force microscopy (AFM) was carried out by using Pucostation STD. To deposit the nanosheets on the substrate, the Si wafer was cleaned successively with methanol/HCl solution and concentrated H₂SO₄, rinsed with deionized water, and dried by high purity N₂ gas. The photoluminescence spectra were measured at room temperature using FP-6600 spectrophotometer (JASCO) with a Xenon flash lamp.

Elemental analysis and thermogravimetry; The ICP analysis data of LRH-Mo (R = Gd and Eu) obtained at different pHs are listed in Table S1.

Table S1. Mo/R molar ratios (R = Gd and Eu) for LRH-Mo obtained at different pHs.

molar ratio	pH			
	~ 4	~ 5	~ 7	~ 9
Mo/Gd	1.30	1.29	0.16	0.10
Mo/Eu	1.27	1.25	0.15	0.10

For the thermogravimetric (TG) analysis, LRH (R = Gd and Eu) and LRH-Mo obtained at pH ~ 4 were heated up to 1000 °C with the rate of 10 °C /min under the N₂ gas flowing condition. Resulting analysis curves are compared in Fig. S1.

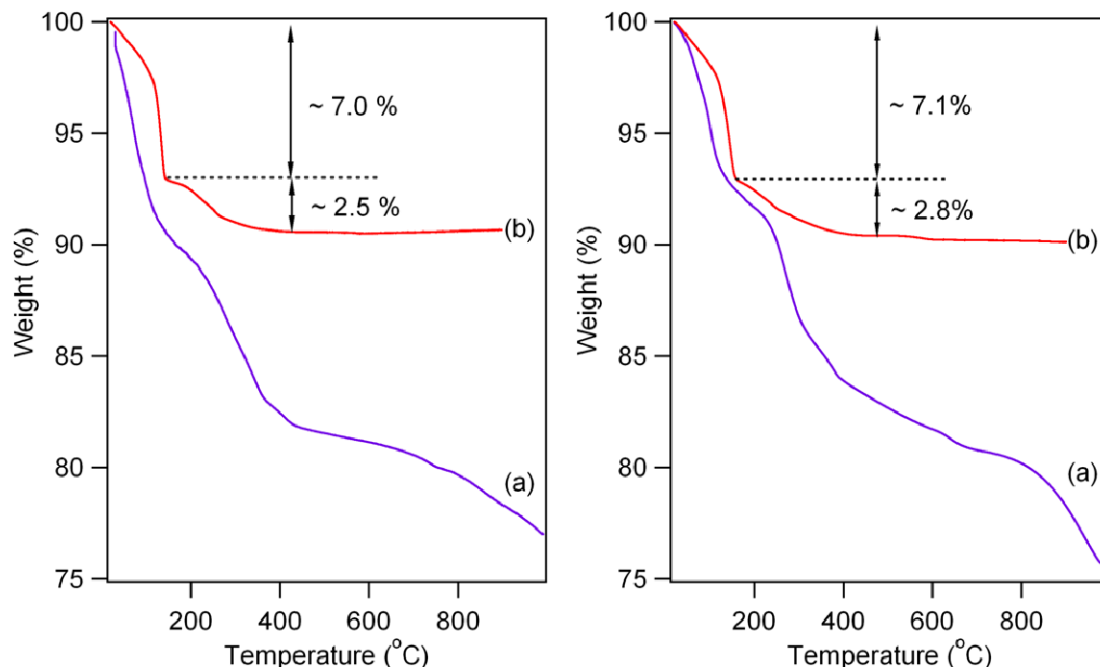


Fig. S1. Thermogravimetric analysis curves for (left, a) LGdH, (left, b) LGdH-Mo precipitate at pH ~ 4, (right, a) LEuH, and (right, b) LEuH-Mo precipitate at pH ~ 4.

TG curves reveal three distinct weight losses. The initial weight loss below 150 °C is due to the removal of water. The amount of interlayer water could be determined from the weight loss in this temperature range. The second weight loss from around 150 to 500 °C is attributed to the loss of water by condensation of hydroxyl groups. A significant different loss between LRH and LRH-Mo evidently indicates that the significant part of hydroxyl groups in the LRH layers were replaced by the polyoxomolybdate groups during the self-assembly process. Therefore, the amount of hydroxyl group in LRH-Mo was determined from the weight loss in this temperature range. The next step higher than 600 °C should involve the loss of Cl₂ which is not observed with LRH-Mo, indicating the absence of residual Cl component after self-assembly. Thermogravimetric analysis and elemental

analysis data proposed the possible chemical formulas $\text{Gd}_{2.00}\text{O}_{0.77}(\text{OH})_{2.24}(\text{Mo}_7\text{O}_{24})_{0.37}\cdot 3\text{H}_2\text{O}$ and $\text{Eu}_{2.00}\text{O}_{0.70}(\text{OH})_{2.44}(\text{Mo}_7\text{O}_{24})_{0.36}\cdot 3\text{H}_2\text{O}$ for LGdH-Mo and LEuH-Mo obtained at pH ~ 4, respectively. The rose-like hierarchical structure is induced at pH lower than 4.5 and, in spite of similar rose shape, its composition can be more or less different depending on the individual pH. As shown in Figure S2, the thermally decomposed products of two compounds were identified to be $\text{R}_2(\text{MoO}_4)_3$ and R_2O_3 ($\text{R} = \text{Gd}$ and Eu) when heated to 1000 °C.

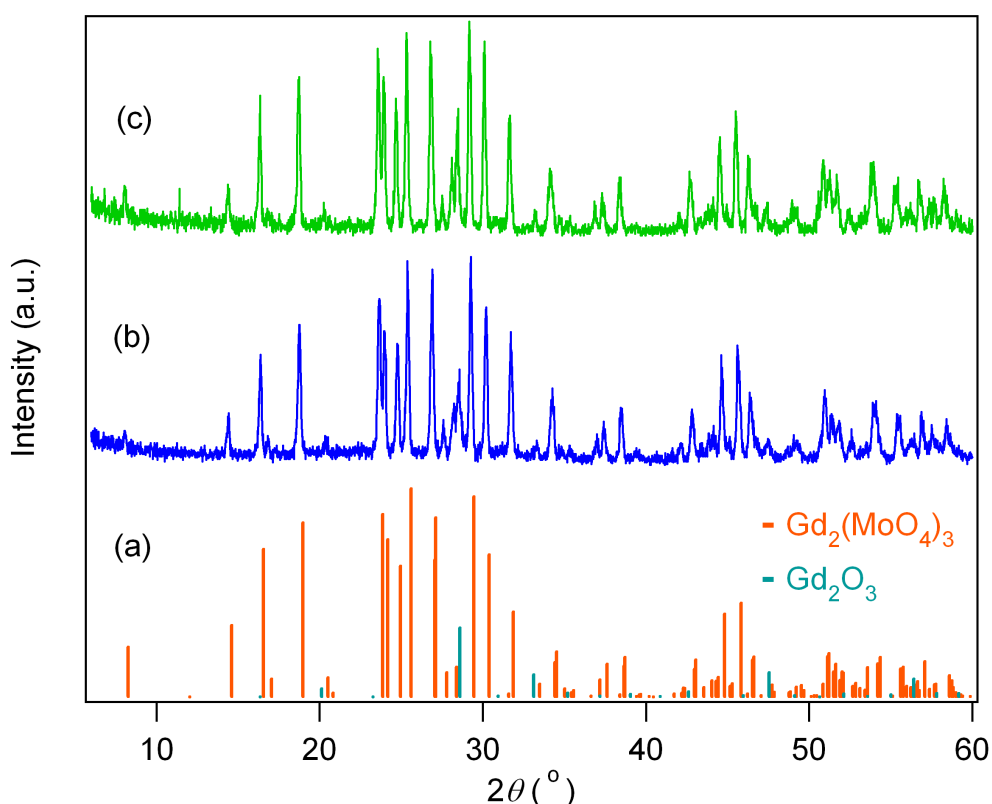


Fig. S2. Comparison of JCPDS cards for (a) $\text{Gd}_2(\text{MoO}_4)_3$ (71-0915) and Gd_2O_3 (86-2477) with XRD patterns of (b) LGdH-Mo and (c) LEuH-Mo after heated at 1000 °C.

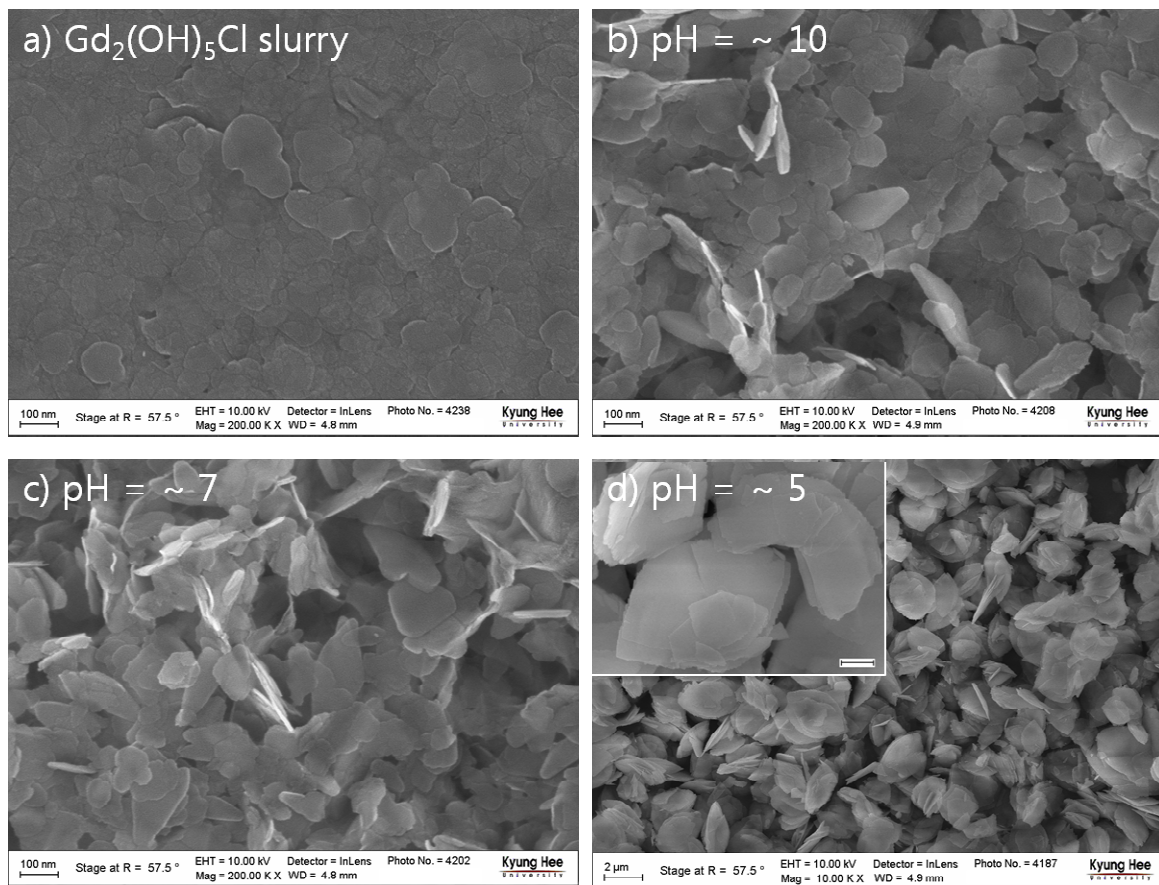


Fig. S3. FE-SEM images of (a) Gd₂(OH)₅Cl·nH₂O slurry (bar = 100 nm) and LGdH-Mo precipitates obtained at pH ~ (b) 10 (bar = 100 nm), (c) 7 (bar = 100 nm), and (d) 5 (bar = 2 μm). Inset: enlarged image (bar = 400 nm).

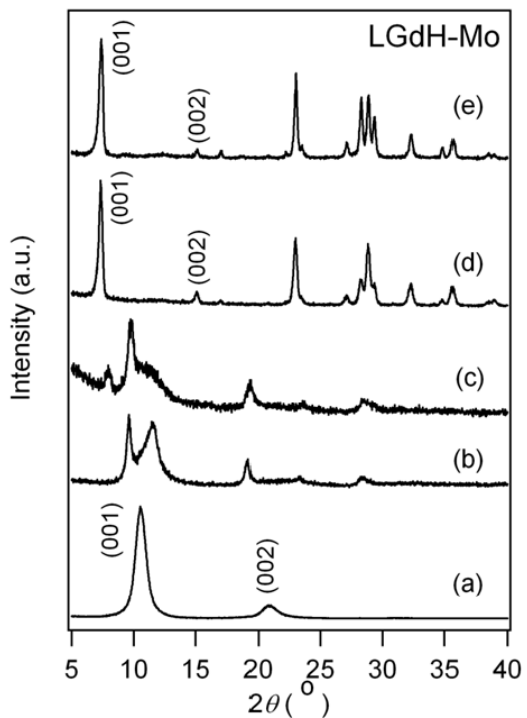


Fig. S4. X-ray diffraction patterns of (a) $\text{Gd}_2(\text{OH})_5\text{Cl}\cdot n\text{H}_2\text{O}$ slurry and LGdH-Mo precipitates obtained at pH ~ (b) 10, (c) 7, (d) 5, and (e) 4.

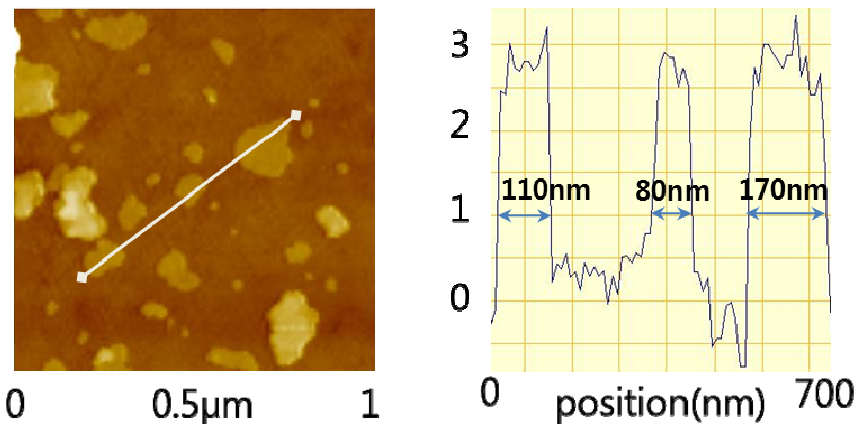


Fig. S5. AFM image and height profile of LGdH sheets deposited on the Si wafer. Based on ca. 0.85 nm of basal spacing for LGdH, the thickness less than 3 nm corresponds to nanosheets composed of 2 to 3 hydroxide layers.

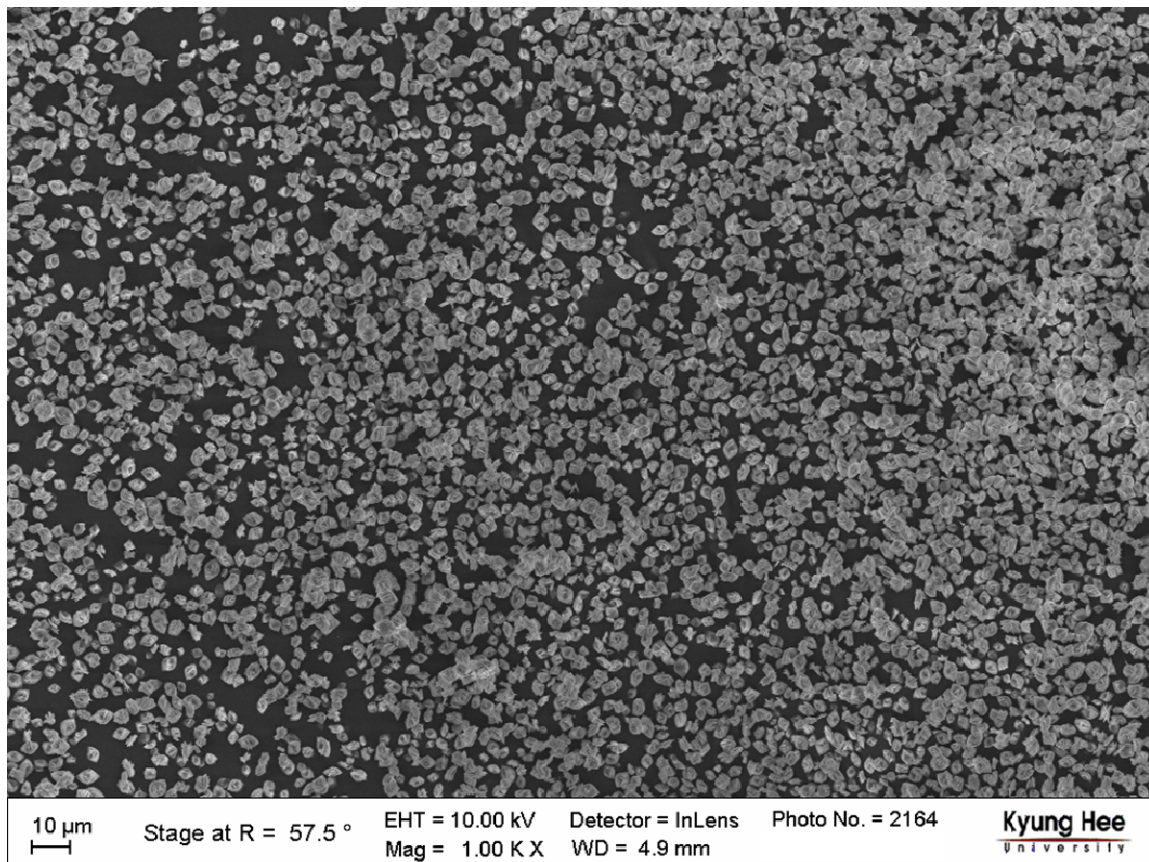


Fig. S6. Low magnification SEM image of LGdH-Mo precipitate at pH ~ 4.

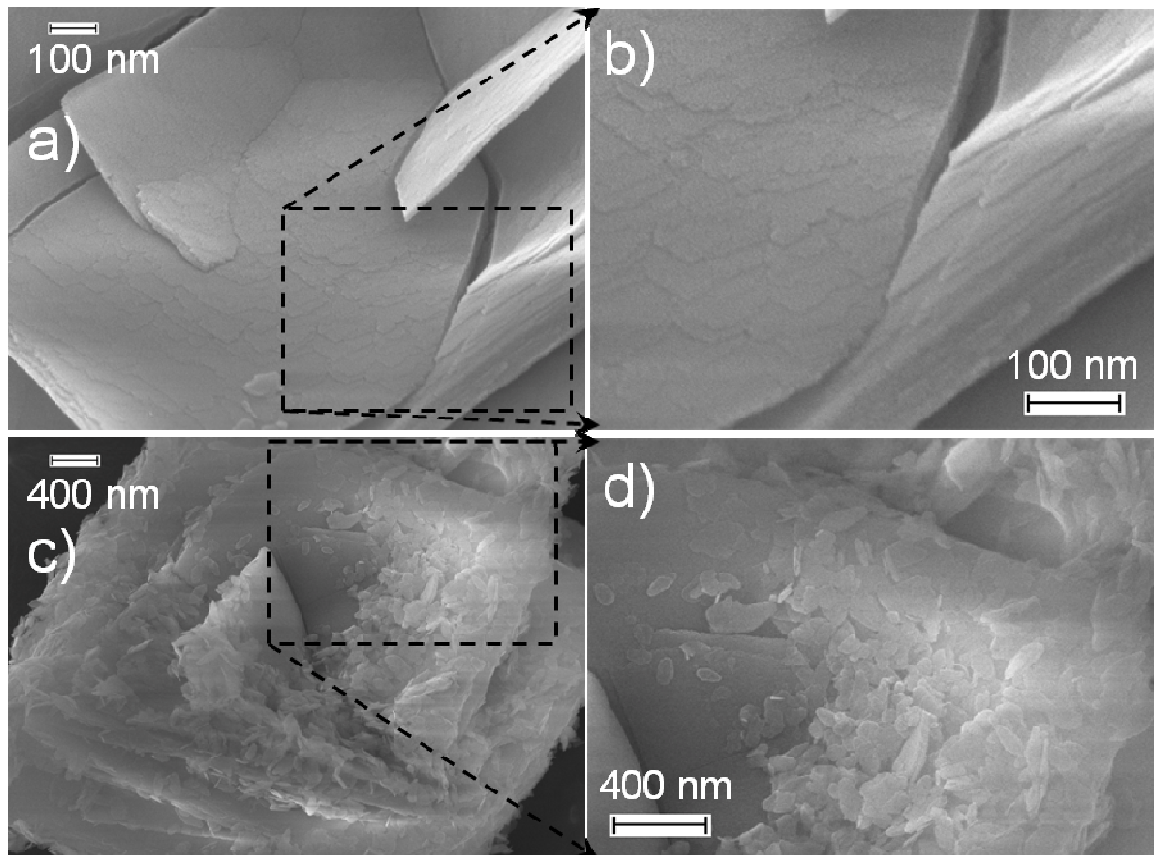


Fig. S7. FE-SEM images of the surface of an individual lamina (petal) formed at (a, b) pH ~ 4 and (c, d) pH ~ 4.6 .

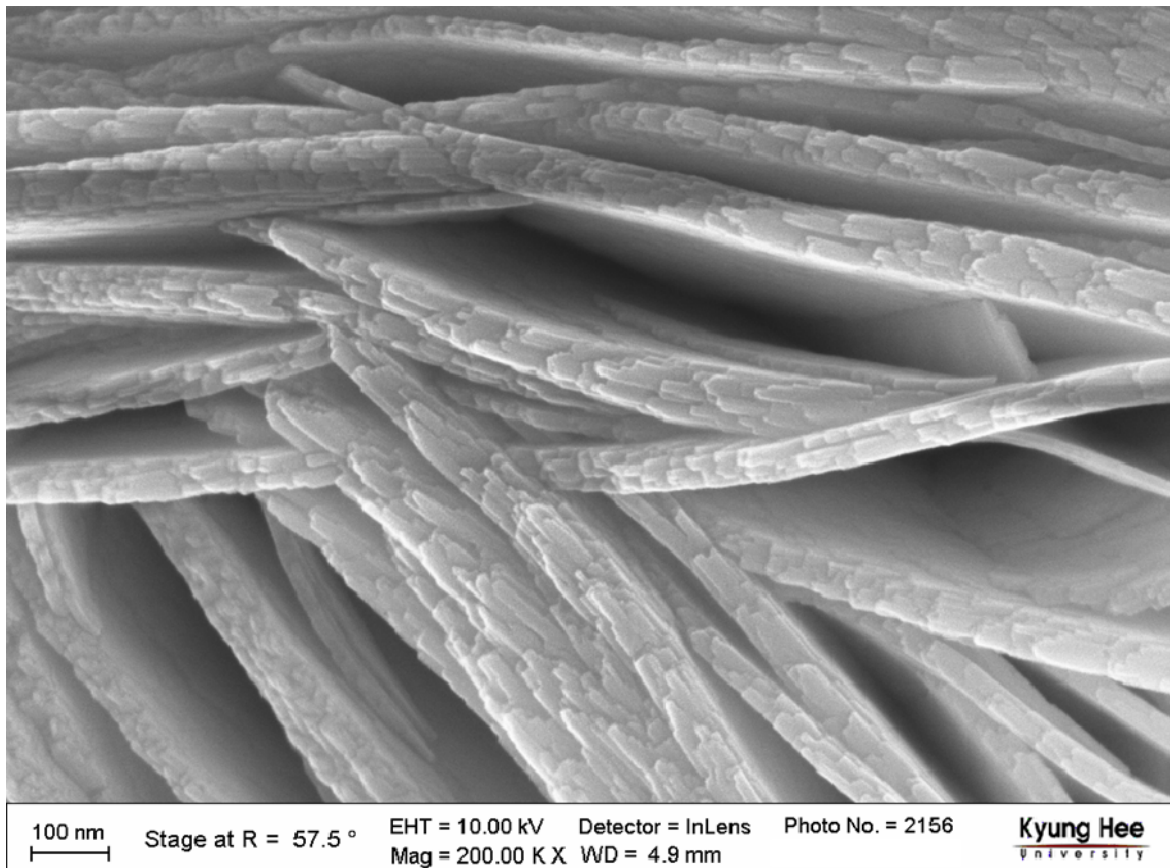


Fig. S8. Side view of the petals of the rose.

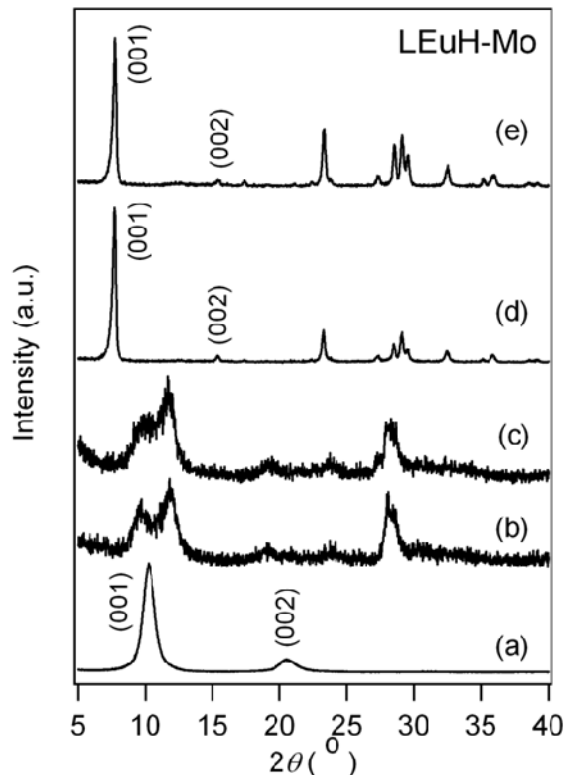


Fig. S9. X-ray diffraction patterns of (a) $\text{Eu}_2(\text{OH})_5\text{Cl}\cdot n\text{H}_2\text{O}$ slurry and LEuH-Mo precipitates obtained at pH ~ (b) 10, (c) 7, (d) 5, and (e) 4.

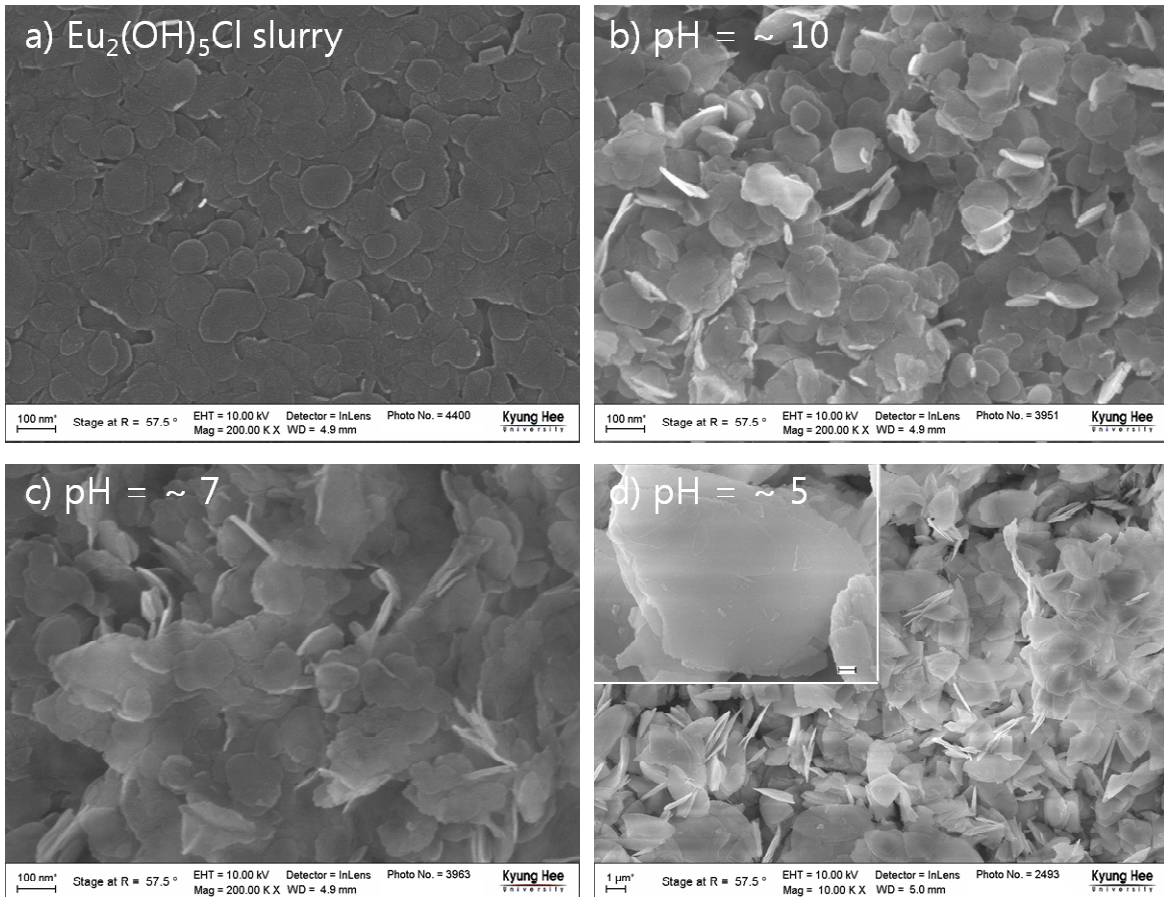


Fig. S10. FE-SEM images of (a) $\text{Eu}_2(\text{OH})_5\text{Cl}\cdot n\text{H}_2\text{O}$ slurry (bar = 100 nm) and LEuH-Mo precipitates obtained at pH ~ (b) 10 (bar = 100 nm), (c) 7 (bar = 100 nm), and (d) 5 (bar = 1 μm). Inset: enlarged image (bar = 200 nm).

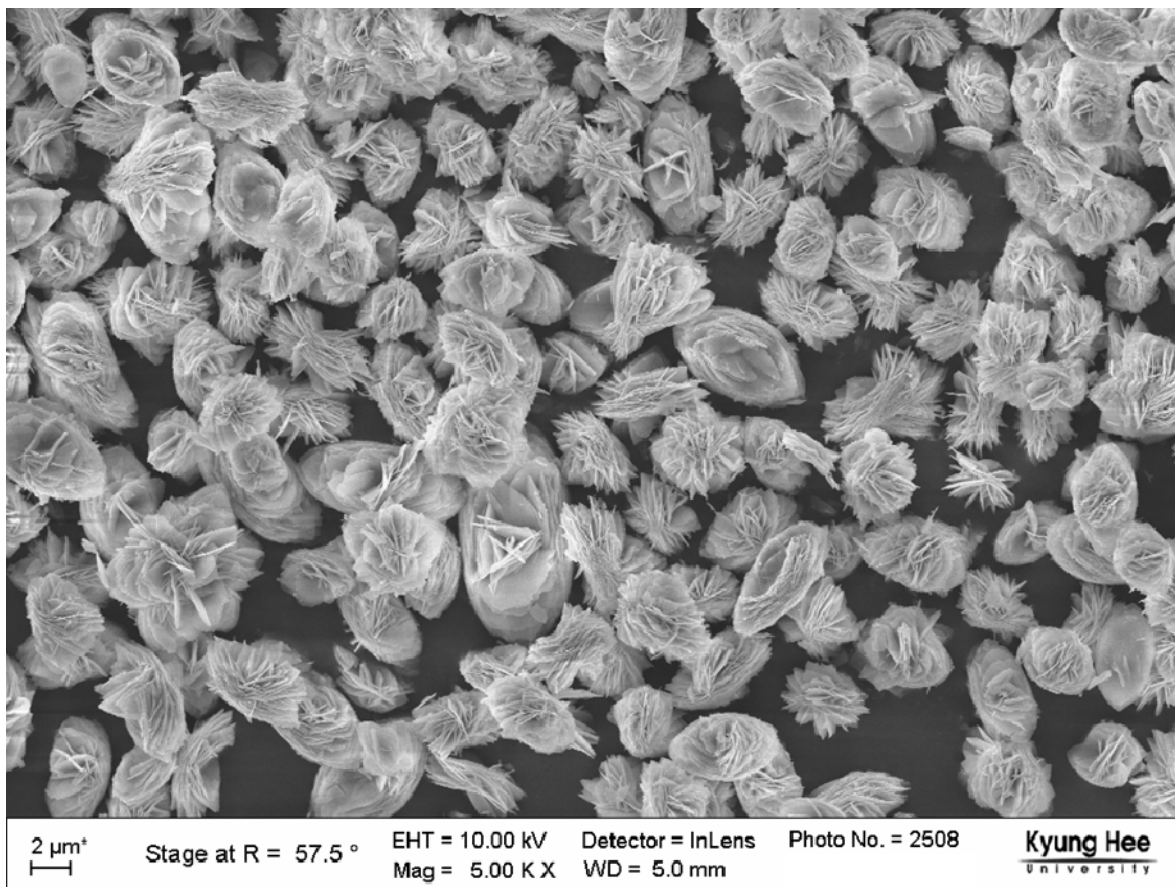


Fig. S11. FE-SEM images of LEuH-Mo powder obtained at pH ~ 4.

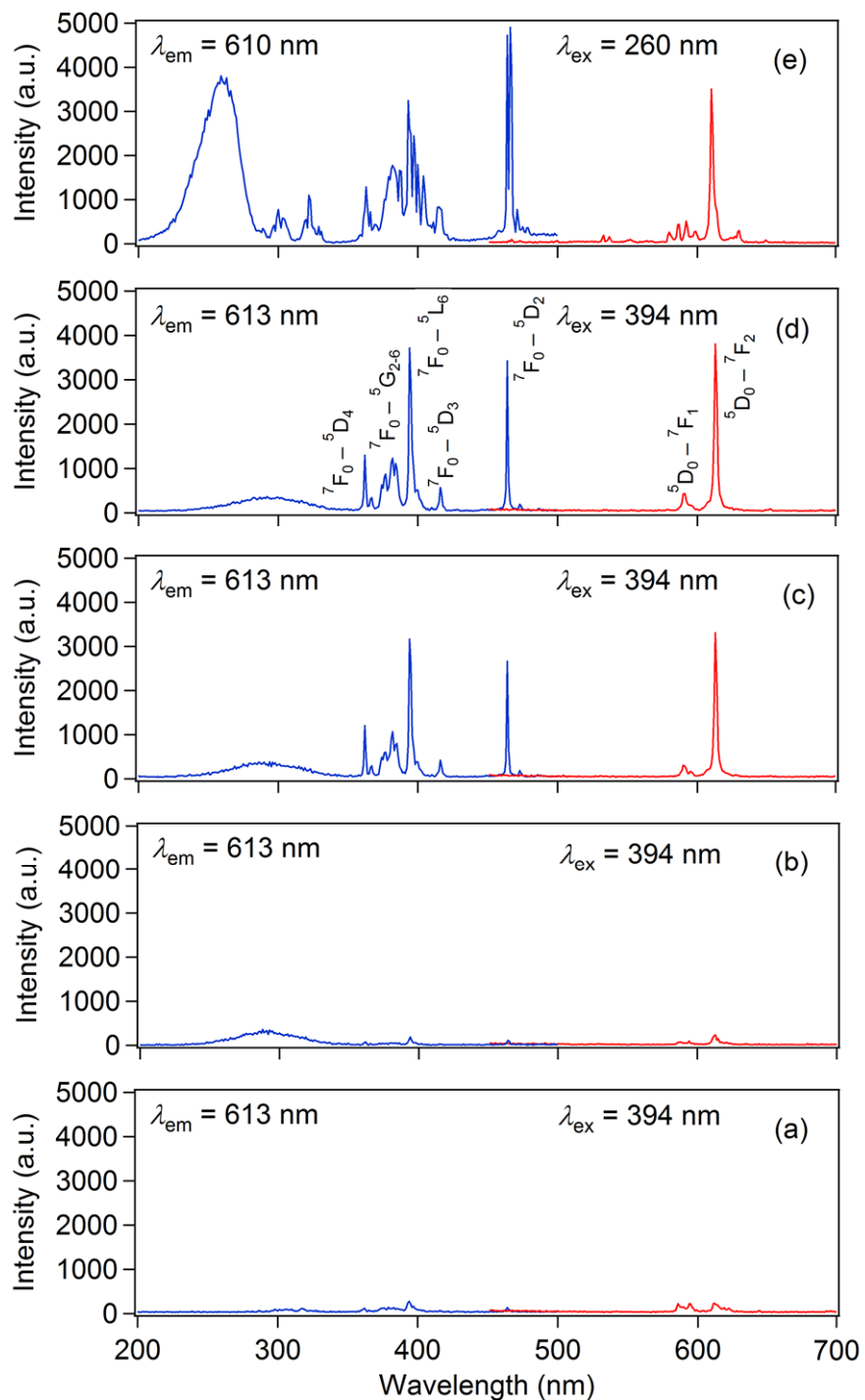


Fig. S12. Excitation (blue) and emission (red) spectra of (a) LEuH and LEuH-Mo precipitates at pH ~ (b) 7, (c) 5, and (d) 4. The PL spectra of commercial Y₂O₃:Eu phosphor (e) are also displayed for comparison. The same weight of samples and reference were measured for relative comparison of intensities.